The Thesis Committee for Nicole Lynn Guckert
Certifies that this is the approved version of the following thesis:

The influence of ankle-foot orthosis stiffness on gait performance in patients with lower limb neuromuscular and musculoskeletal impairments

APPROVED BY
SUPERVISING COMMITTEE:

Supervisor:

Richard R. Neptune

Richard H. Crawford

The influence of ankle-foot orthosis stiffness on gait performance in patients with lower limb neuromuscular and musculoskeletal impairments

by

Nicole Lynn Guckert, B.S.Biomed.E.

Thesis

Presented to the Faculty of the Graduate School of

The University of Texas at Austin

in Partial Fulfillment

of the Requirements

for the Degree of

Master of Science in Engineering

The University of Texas at Austin

December 2012

Acknowledgements

I would like to thank Dr. Richard Neptune for his continued guidance and support as my research advisor. In addition, I would like to thank our collaborators at the Center for the Intrepid in Fort Sam Houston, TX, Dr. Jason Wilken, Dr. Deanna Gates, Dr. Elizabeth Russell, Jennifer Aldridge and Kelly Rodriguez for their help with subject recruitment and data collection. I would also like to thank Dr. Allison Hall and Dr. Nick Fey for their help with selective laser sintering and Dr. Richard Crawford for his feedback in the preparation of this thesis.

In addition, I would like to thank my fiancé, Austin, for his continued love and support and my adorable cat Nox for sleeping on my keyboard when he knew I needed a break. Lastly, I would also like to thank my mom, dad and sister who have provided me with the support and love that has been so monumental in each of my accomplishments.

This study was supported in part by a National Science Foundation Graduate Research Fellowship, Cockrell School of Engineering Fellowship and a research grant from the Center for Rehabilitation Sciences Research. The contents are solely the responsibility of the author and do not necessarily represent the official views of The University of Texas at Austin, the National Science Foundation, or the Center for Rehabilitation Sciences Research.

Abstract

The influence of ankle-foot orthosis stiffness on gait performance in patients with lower limb neuromuscular and musculoskeletal impairments

Nicole Lynn Guckert, M.S.E.

The University of Texas at Austin, 2012

Supervisor: Richard R. Neptune

Individuals with various lower-limb neuromuscular and musculoskeletal impairments are often prescribed passive-dynamic ankle-foot orthoses (PD-AFOs) to compensate for impaired ankle muscle weakness. Several studies have demonstrated the beneficial effects of PD-AFOs on pathological gait, but few studies have examined the influence of the AFO stiffness characteristics on gait performance. One challenge to performing such studies is the difficulty of manufacturing custom AFOs with a wide range of controlled stiffness levels. However, selective laser sintering (SLS) is a well-suited additive manufacturing technique for generating subject-specific PD-AFOs of varied stiffness. Therefore, the overall goal of this study was to use SLS manufactured PD-AFOs to identify the relationships between AFO stiffness and gait performance in patients with various lower-limb neuromuscular and musculoskeletal impairments. Six subjects with unilateral impairments were enrolled in this study. For each subject, one subject-specific PD-AFO equivalent to the subject's clinically prescribed carbon fiber

PD-AFO (nominal), one 20% more compliant and one 20% more stiff were manufactured using SLS. Three-dimensional kinematic and kinetic data were collected from each subject while ambulating with each PD-AFO at two different speeds to allow a comprehensive biomechanical analysis to assess the influence of PD-AFO stiffness on gait performance. The results showed that in the compliant AFO condition, the AFO limb vertical ground reaction force (GRF) impulse during loading and the non-AFO limb medial GRF impulse during push-off decreased. In addition, the AFO limb braking GRF impulse during loading and the non-AFO limb braking GRF impulse in early single-limb stance decreased. Furthermore, in the compliant AFO condition, negative knee work during early single-limb stance increased while positive hip work in early swing decreased in the AFO limb. Overall, as AFO stiffness decreased, the AFO limb contributed less to body support and braking. In addition, a decreased medial GRF impulse coupled with an increased vertical GRF impulse during non-AFO single-limb stance suggests that walking stability may be compromised as AFO stiffness decreases. Thus, a tradeoff may exist between preserving stability and increasing net propulsion, which should be considered when assessing the mobility needs of individuals prescribed PD-AFOs as a result of various neuromuscular and musculoskeletal impairments.

Table of Contents

List of Tables

List of Figures

Introduction

Individuals with various lower-limb neuromuscular and musculoskeletal impairments often experience ankle muscle weakness (Goldberg and Hsu, 1997). Ankle muscle weakness greatly affects walking ability as the plantarflexor and dorsiflexor muscles have been shown to be important contributors to body support, forward propulsion (Liu et al., 2006; Neptune et al., 2001), leg swing initiation (Neptune et al., 2001), mediolateral balance control (Allen and Neptune, 2012; Pandy et al., 2010) and foot clearance during swing. As a result, ankle-foot orthoses (AFOs) are commonly prescribed to facilitate gait in patients with these impairments by mechanically compensating for ankle weakness (Dvorznak et al., 2007). Studies have shown various traditional AFOs, including rigid and articulating AFOs, have a number of positive effects on gait including promoting normal toe clearance during swing (e.g., Bregman et al., 2010; Buckon et al., 2004; Gok et al., 2003; Lehmann et al., 1986), improving spatiotemporal parameters of gait (e.g., Bregman et al., 2010; Buckon et al., 2004; Buckon et al., 2001; de Wit et al., 2004; Gok et al., 2003; Lehmann et al., 1985; Tyson and Thornton, 2001), decreasing the energy cost of walking (e.g., Bregman et al., 2010; Buckon et al., 2004), promoting heel strike (e.g., Buckon et al., 2004; Buckon et al., 2001; Gok et al., 2003), facilitating forward progression (e.g., Lehmann et al., 1985), and improving medial-lateral stability (e.g., Lehmann et al., 1986) and balance (for review, see Ramstrand and Ramstrand, 2010).

Passive-dynamic AFOs (PD-AFOs) are a class of AFOs that rely on design characteristics to further improve gait performance through elastic energy storage and return (ESAR) (Faustini et al., 2008). Although several studies have demonstrated the beneficial effects of carbon fiber PD-AFOs on pathological gait compared to walking

without an AFO (Danielsson and Sunnerhagen, 2004; Desloovere et al., 2006; Patzkowski et al., 2012; Van Gestel et al., 2008) or with traditional AFOs (Bartonek et al., 2007; Desloovere et al., 2006; Patzkowski et al., 2012; Van Gestel et al., 2008; Wolf et al., 2008), few studies have examined the influence of the stiffness characteristics on gait performance. Two studies that have investigated the influence of AFO stiffness found that stiffness could affect the energy cost of walking (Bregman et al., 2011) and influence joint kinematics (Kobayashi et al., 2011, 2012). In addition, recent studies that have varied the stiffness characteristics of foot-ankle prosthetic devices found that as stiffness decreased the prosthesis contributed less to body support, which necessitated an increase in the activity of muscles that contribute to body support, specifically the vasti and rectus femoris (Fey et al., 2011; Ventura et al., 2011a, b). The increased vasti and rectus femoris activity resulted in increased knee extensor moments (Fey et al., 2011; Ventura et al., 2011b). These studies also showed that as stiffness decreased, the prosthesis' contribution to forward propulsion increased resulting in a decrease in the hamstring muscle activity, which normally contributes to forward propulsion (Fey et al., 2011; Ventura et al., 2011a, b). One of these studies also found that as stiffness decreased, prosthesis energy storage in early and mid-stance and energy return in late stance increased (Fey et al., 2011). However, no study has systematically investigated the influence of PD-AFO stiffness on specific biomechanical variables such as ground reaction forces and joint kinematics and kinetics.

One challenge to performing such studies is the difficulty of manufacturing custom AFOs with a wide range of controlled stiffness levels. Previous studies have adjusted stiffness through fluid mechanics (Kobayashi et al., 2011; Yamamoto et al., 2005; Yokoyama et al., 2005), springs (Yamamoto et al., 1999), elastic components (Bleyenheuft et al., 2008) and design (Desloovere et al., 2006), but these techniques

provided stiffness levels that were either difficult to precisely control or limited to a few discrete levels of resistance at the AFO hinge. An alternative approach is to use selective laser sintering (SLS), which is an additive manufacturing technique that facilitates more automated fabrication of custom PD-AFOs and gives the user more precise control over design characteristics such as stiffness. SLS has recently been use to create PD-AFOs (Faustini et al., 2008; Schrank and Stanhope, 2011), foot orthoses (Pallari et al., 2010), prosthetic sockets (Faustini et al., 2006; Rogers et al., 2008; Rogers et al., 2007), prosthetic feet (Fey et al., 2011) and prosthetic ankles (Ventura et al., 2011a, b).

Therefore, the overall goal of this study was to use SLS PD-AFOs to identify the relationships between AFO stiffness and gait performance in patients with lower-limb neuromuscular and musculoskeletal impairments due to various limb salvage procedures. We hypothesize that as AFO stiffness decreases: 1) AFO limb ankle range of motion (ROM) and work will increase due to increased elastic energy storage and return; 2) the AFO's contribution to body support will diminish, as indicated by a decrease in the vertical GRF impulses, and thus knee extensor moments and subsequently knee work will increase to compensate; 3) the AFO's contribution to forward propulsion will increase, as indicated by an increase in the propulsive GRF impulses, and thus hip extensor moments and subsequently hip work will decrease as a result. Through assessment of these hypotheses, the results will help guide the development of more effective AFO designs and quantitative prescription criteria for PD-AFOs.

Methods

Subject-specific PD-AFOs of varying stiffness characteristics were created using Selective Laser Sintering (SLS). Each subject's clinically prescribed PD-AFO was a modular, carbon fiber (CF) design consisting of a footplate, cuff and posterior strut (Intrepid Dynamic Exoskeletal Orthosis, Brooke Army Medical Center, San Antonio, TX; Figure 1). The AFO stiffness was modified by altering the geometry of the posterior strut. A SLS strut with stiffness equivalent to the CF strut was designed and manufactured for each patient as well as SLS struts that were 20% more compliant and 20% more stiff than the CF strut. The stiffness of each SLS strut was verified post-build by performing a three-point-bend test and destructive testing was performed on duplicate struts to ensure their structural integrity. The struts were then evaluated on subjects during overground walking trials to quantify the effects of PD-AFO stiffness on gait performance. The methods are described below in detail. From this point forward the PD-AFOs will be referred to as AFOs for brevity.

Figure 1. Clinically prescribed carbon fiber (CF) PD-AFO (Intrepid Dynamic Exoskeletal Orthosis, Brooke Army Medical Center, San Antonio, TX).

SUBJECTS

Six active military personnel with unilateral lower extremity injuries and resulting ankle muscle weakness participated in this study (Table 1). All subjects were asymptomatic of musculoskeletal disorders affecting the contralateral limb. Each subject had been prescribed an Intrepid Dynamic Exoskeletal Orthosis (Patzkowski et al., 2012) by their orthopedic surgeon and provided institutionally approved written informed consent prior to their participation in this study. All subject data were collected in the Military Performance Laboratory at the Center for the Intrepid in Fort Sam Houston, TX.

Table 1. Characteristics for subjects with unilateral neuromuscular and musculoskeletal impairments due to various limb salvage procedures and resultant ankle muscle weakness.

	Mean	Std. Dev.	Max	Min	# Subjects
Age (years)	29.83	6.08	40.00	21.00	-
Height (m)	1.80	0.06	1.92	1.75	-
Body Mass (kg)	87.95	9.39	97.30	78.2	-
Leg Length (m)	1.02	0.06	1.14	0.95	-
Gender					
Male	-	-	-	-	6
Female	-	-	-	-	0
Affected Limb					
Right	-	-	-	-	3
Left	-	-	-	-	3

DESIGN AND MANUFACTURE OF THE SLS AFOS

The primary elements of the SLS framework used to create the subject-specific struts included: (1) mechanically testing the subject's clinically prescribed CF strut to determine its stiffness, (2) using computer-aided design (CAD) to develop struts that were 20% more stiff, 20% more compliant and equivalent to the CF strut stiffness, (3) fabricating the struts using SLS, (4) mechanically testing each strut to verify the stiffness, and (5) performing mechanical testing of tensile specimens and destructive testing of duplicates of each strut to ensure their structural integrity.

The stiffness of each subject's prescribed AFO was determined through mechanical testing of the posterior CF strut in a three-point-bend configuration using a mechanical testing machine with a 5000 N uniaxial load cell (Instron, Norwood, MA). A load of 890 N (200 lbf) was applied at a rate determined by the ASTM standard D790 as follows:

$$R = \frac{z * L^2}{6 * d} \quad (1)$$

where R is the loading rate (mm/min), z is the rate of straining of the specimen outer fiber (0.01 mm/mm/min), L is the length of support span (mm), and d is the depth of specimen (mm). The resulting deflection was used to calculate the stiffness.

Nylon 11 powder (PA D80-ST, Advanced Laser Materials, Temple, TX), which has high ductility and low damping properties (Faustini et al., 2008), was used in the SLS process. To achieve the desired stiffness characteristics while satisfying other design constraints, the strut geometry was modified to a channel beam design (Figure 2) and the stiffness was varied by altering the strut thickness. Design constraints included maintaining a uniform stiffness along the length of the strut, minimizing the thickness at the bolt holes without introducing a stress concentration point, minimizing the overall thickness, and maintaining a width of less than 4.5 cm.

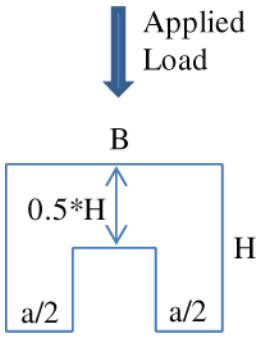

Figure 2. Cross-sectional geometry of the channel beam SLS AFO strut and the direction of loading during the three-point-bend test and when the AFO is on the subject. 'H' is the AFO strut thickness, 'a' is the difference between the total width and the channel width, and 'B' is the total width.

A generic SLS strut satisfying these constraints was designed in Solidworks (SolidWorks, Waltham, MA) and finite element analysis (FEA) simulations were performed to assess and minimize the stresses within the strut under physiologic loads. A predictive model for stiffness was developed by manufacturing a series of SLS struts of

varying thicknesses. Stiffness was predicted using the equation for the area moment of inertia (*I*) of the channel beam depicted in Figure 2 (Eq. 2) as well as the equation for deflection in a three-point-bend test (Eq. 3) as follows:

$$I = \frac{1}{24}(a + B)H^3 \qquad mm^4 \tag{2}$$

$$I = \frac{55567.89}{f} \qquad mm^4 \tag{3}$$

where *a* is the difference between the total width and the channel width (mm), *B* is the total width (mm), *H* is the thickness of the strut (mm), and *f* is the deflection of the strut (mm). After manufacturing struts with a range of stiffness values, it was determined that a scaling factor for the area moment of inertia was necessary to successfully predict the SLS strut stiffness because the area moment of inertia specified in Eq. 2 was based on the geometry of a channel beam and the AFO strut design varied in small ways (e.g. fillets) from a strict channel beam design. A linear model to predict the necessary scaling factor (*SF*) from the desired stiffness was developed from experimental data as follows:

$$SF = 0.003(k) + 0.7494 \tag{4}$$

where *k* is the desired stiffness of the SLS strut in units of kgf/mm. Through combining equations (2) – (4), a thickness was calculated for each strut to obtain the desired stiffness. The generic AFO strut CAD model was modified in Solidworks for each subject to match the length of the CF strut and incorporate the desired thickness for each stiffness condition.

The Solidworks CAD files were then exported to a Vanguard HiQ/HS Sinterstation (3D Systems, Inc., Rock Hill, SC) using the STL file format. During the SLS process, the 3D model of the strut is mathematically sliced into thin, planar, cross-sectional geometries. To build each cross-section, a 0.004 inch layer of powder is distributed evenly over a part bed and sintered together in the desired cross-sectional shape using a high-powered scanning laser beam. After lowering the part bed and depositing a new layer of powder, the next cross-section is sintered to the previous layer. Successive cross-sections are sintered layer-by-layer until the final part, possessing the same dimensions and shape as the CAD model, is complete. The AFO struts were built with the channels oriented downward so that if within-build curling occurred the AFO strut would curl in the direction that caused increased dorsiflexion, which can be corrected for with a wedge during patient fitting. A duplicate of each strut was built adjacent to the original to ensure uniform material properties for the destructive testing. In addition, tensile specimens, designed according to the ASTM standard D638, were manufactured throughout the build volume (e.g. on the top, on the bottom and vertically every 0.5 inches of the build) to assess the uniformity of part properties throughout the entire build volume.

After the struts were manufactured, mechanical testing was performed on each strut in the same three-point-bend configuration used to test the CF struts. Tensile testing was performed on each tensile specimen to assess their material properties using ASTM standard D638. If all tensile specimens exhibited percent elongations greater than 20% and Young's Moduli within the range of 1300 to 1800 MPa, then destructive testing was performed on one strut from each identical pair. Destructive testing of each strut was performed using a three-point-bend configuration on a mechanical tester with a 100 kN uniaxial load cell (MTS ReNew/Instron, Eden Prairie, MN). The strut was loaded at 500

mm/min (maximum rate) until it fractured or was plastically deformed past the ultimate flexural strength. If the strut did not fracture during destructive testing and if all tensile specimens indicated the parts had appropriate ductility and strength, then the paired strut was deemed safe for use in the overground walking trials.

EXPERIMENTAL WALKING PROTOCOL

The experimental protocol was a crossover design in which the subjects underwent four biomechanical gait assessments in a randomized order, one for each AFO strut (CF strut, nominal SLS strut, 20% more stiff SLS strut and 20% more compliant SLS strut). Prior to testing each AFO, a certified orthotist attached the strut to the cuff and footplate and ensured proper alignment. Subjects were given time to acclimate to each new device until they were comfortable for testing. In addition, Clubmaker™ lead tape (Golfsmith, Austin, TX) was affixed to the CF, nominal, and compliant struts to match the weight of the stiff SLS strut.

Subjects walked overground on a walkway with 5 embedded forceplates at their self-selected velocity (SS) and a controlled velocity (Froude velocity). The Froude velocity (*FR*), which enables dynamically equivalent comparisons across subjects, was calculated on the basis of an individual subject's leg length as:

$$FR = N_{fr}\sqrt{g * l} \tag{5}$$

where *FR* is the Froude velocity, N_{fr} is the Froude number (0.40 for this study), g is gravitational acceleration, and l is leg length measured as the distance from the greater trochanter to the floor while the subject was standing (Vaughan and O'Malley, 2005).

For the Froude velocity, auditory cues (Biofeed Trak, Motion Analysis Corp., Santa Rosa, CA) based on trunk marker velocity were used to provide speed feedback to the subjects. For each condition, subjects walked over the embedded forceplates until at least 10 forceplate strikes were collected for each leg. A forceplate strike was defined as contact occurring between only one foot and one forceplate for the entire stance phase.

Ground reaction force (GRF) data were collected from the 5 embedded AMTI forceplates (AMTI, Inc., Watertown, MA) at 1200 Hz. A 6 degree-of-freedom body segment marker set (Collins et al., 2009; Manal et al., 2000; Wilken et al., 2012) and an optoelectronic motion capture system (Motion Analysis Corp., Santa Rosa, CA) comprising 26 cameras operating at 120 Hz were used to collect 3D whole body kinematics. Reflective markers were placed on the C-7 vertebra, sternal notch, xyphoid process, T-8 vertebra, the right scapula and bilaterally on the forehead, back of the head, acromium process, proximal and posterior upper arm, anterior upper arm, distal and posterior upper arm, medial and lateral forearm, radial styloid, ulnar styloid, third metacarpal head, anterior superior iliac spine, iliac crest, posterior superior iliac spine, heel, second metatarsal head, fifth metatarsal head and lateral heel. Marker clusters consisting of four markers each were placed bilaterally on the shank and thigh. A digitization process was used to identify 20 bilateral anatomical bony landmarks including the anterior and posterior aspects of the glenohumeral joint, medial and lateral humeral epicondyles, medial and lateral femoral epicondyles, medial and lateral malleoli, greater trochanters and iliac crests.

KINEMATICS AND KINETICS

Using Visual3D (C-Motion, Inc., Germantown, MD), marker trajectory data were interpolated using a cubic polynomial and ground reaction force and marker trajectory data were filtered using a 4^{th}-order butterworth filter with cutoff frequencies of 50 and 6 Hz, respectively. A 13-segment model consisting of a head, torso, pelvis, two upper arms, two lower arms, two thighs, two shanks and two feet was created and scaled to each subject's body weight and height. Anatomical landmarks were used to define joint centers as well as joint coordinate systems using the International Society of Biomechanics (ISB) standards (Grood and Suntay, 1983; Wu and Cavanagh, 1995; Wu et al., 2002). Sagittal plane kinematics were computed using an Euler angle approach with ankle and hip cardan sequences defined by ISB standards (Wu et al., 2002), the knee joint cardan sequence defined by Grood et al. (Grood and Suntay, 1983) and the pelvis cardan sequence defined by Baker (Baker, 2001). Inverse dynamics analysis was performed to calculate net intersegmental joint moments and powers which were expressed in the proximal segment coordinate system. GRFs were normalized by subject body weight and joint moments and powers were normalized by subject body mass. Spatiotemporal gait characteristics were determined in Visual3D. GRFs as well as sagittal plane joint angles, moments and powers corresponding to each forceplate strike were time-normalized to a full gait cycle and exported for further analysis in Matlab (MathWorks, Inc., Natick, MA).

In Matlab, the data were further analyzed by dividing the gait cycle into six regions (Figure 3). For the AFO limb, these six regions were defined as 1) loading (AFO heel-strike to non-AFO toe-off), 2) early single-leg support and 3) late single-leg support (non-AFO toe-off to non-AFO heel-strike divided into two equal sections), 4) push-off (non-AFO heel-strike to AFO toe-off), 5) early swing and 6) late swing (AFO toe-off to

AFO heel-strike divided into two equal sections). For each region of the gait cycle, peak values were identified for each kinematic and kinetic variable of interest and work and GRF impulses were calculated. Work at the ankle, knee and hip was computed as the time integral of the corresponding joint power curve within each of the six regions of the gait cycle. GRF impulses were computed as the time integral of the anterioposterior (A/P), mediolateral (M/L) and vertical GRF curves within each of the six regions of the gait cycle. In addition, the unloaded AFO angle was subtracted from the AFO limb ankle angle to minimize any biasing due to variations in AFO strut alignment. For each subject, variables of interest were averaged across all gait cycles for each combination of stiffness condition and velocity.

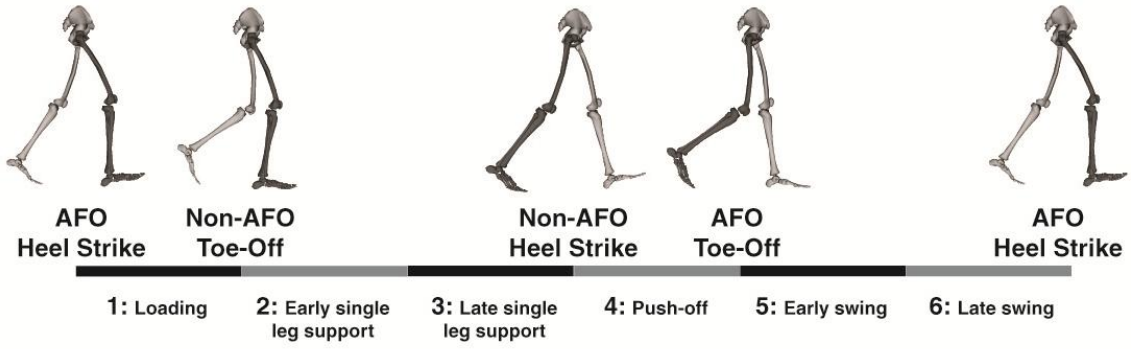

Figure 3. The six regions of the AFO limb gait cycle: 1) loading, 2) early single-limb stance, 3) late single-limb stance, 4) push-off, 5) early swing and 6) late swing.

STATISTICAL ANALYSES

A number of statistical analyses were performed using SPSS 16.0 (SPSS, Inc.) to test the hypotheses. To test the first hypothesis that the AFO limb ankle range of motion and work would increase as AFO stiffness decreased, differences in peak ankle angles

and moments during the stance phase of the gait cycle (Regions 1-4) and differences in ankle joint work in each of the six regions of the gait cycle were analyzed using two-factor (AFO stiffness, leg) repeated-measures ANOVAs. To test the second hypothesis that the AFO's contribution to body support would diminish and knee joint work and knee extensor moments would increase to compensate as AFO stiffness decreased, differences in vertical GRF impulses and peak knee angles and moments during the stance phase of the gait cycle (Regions 1-4) and differences in knee joint work in each of the six regions of the gait cycle were analyzed using two-factor (AFO stiffness, leg) repeated-measures ANOVAs. The final hypothesis that the AFO's contribution to forward propulsion would increase and thus hip joint work and hip extensor moments would decrease as AFO stiffness decreased was tested by analyzing the differences in braking and propulsive GRF impulses and peak hip angles and moments during the stance phase of the gait cycle (Regions 1-4) and differences in hip joint work in each of the six regions of the gait cycle using two-factor (AFO stiffness, leg) repeated-measures ANOVAs. In addition, differences in medial and lateral GRF impulses were assessed during the stance phase of the gait cycle (Regions 1-4) using two-factor (AFO stiffness, leg) repeated-measures ANOVAs. The AFO stiffness factor consisted of four levels (CF, nominal SLS, 20% more stiff SLS and 20% more compliant SLS) while the leg factor consisted of two levels (AFO and non-AFO). Significant main or interaction effects resulting from these ANOVAs were adjusted using a Huynh-Feldt correction. Pairwise comparisons among AFO conditions were evaluated with a Bonferroni correction for multiple comparisons.

Results

SLS-Manufactured AFO Struts

The SLS framework successfully generated struts matching the desired stiffness levels. For each of the six subjects, all three struts matched the desired stiffness levels within ± 5% (Table 2). In addition, all duplicate struts passed the destructive testing without fracturing. Forces ranging from 517 kgf (Subject 2: compliant) to 1252 kgf (Subject 6: stiff) were achieved during destructive testing as the strut plastically deformed past the ultimate flexural strength.

Table 2. Stiffness of SLS-Manufactured AFO struts and % difference from the desired stiffness for each condition: Carbon Fiber (CF), Nominal SLS, Compliant SLS, and Stiff SLS.

	CF Strut Stiffness (kgf/mm)	Nominal Strut Stiffness (kgf/mm)	% Diff from Desired	Compliant Strut Stiffness (kgf/mm)	% Diff from Desired	Stiff Strut Stiffness (kgf/mm)	% Diff from Desired
Subject 1	87.90	85.35	2.90	69.57	1.06	101.80	3.49
Subject 2	49.95	52.12	4.34	40.84	2.19	61.33	2.31
Subject 3	57.65	57.46	0.32	45.67	0.97	69.87	1.01
Subject 4	77.69	75.69	2.57	60.33	2.92	89.30	4.21
Subject 5	62.68	63.05	0.59	49.39	1.51	75.00	0.29
Subject 6	94.91	95.01	0.11	76.90	1.28	112.90	0.87

Spatiotemporal Data

Overall there was large variability in the spatiotemporal characteristics for all six subjects (Appendix: Table A1 and A2). Despite this variability, similarities in several spatiotemporal gait parameters (specifically in Subjects 3-6), such as average speed, average double support time and average step time for the AFO limb, were observed

during walking with the CF and nominal AFOs (Appendix: Table A1 and A2). High inter-subject variability obscured differences between conditions and velocities; however, as stiffness decreased some trends were observed for subgroups of subjects.

Three subjects at their FR exhibited decreased average stride width as stiffness decreased (Table A1: FR - Subjects 1, 5, and 6). In addition, for two subjects, average step length of the AFO limb increased at their FR while average step length of the non-AFO limb increased at their SS as stiffness decreased (Table A1: FR and SS - Subjects 1 and 6).

In two subjects, as stiffness decreased average step time of the AFO limb decreased at both velocities (Table A2: FR - Subjects 5 and 6, SS - Subjects 1 and 3) while the average step time of the non-AFO limb increased at their FR (Table A2: FR - Subjects 2 and 3). In addition, at their FR two of the six subjects had decreased average double support time (Table A2: FR - Subjects 4 and 6) as stiffness decreased.

JOINT ANGLES

Decreasing AFO stiffness had a minimal effect on the knee and hip angles. At both velocities (FR – Figure 4; SS – Figure 5) the ankle of the non-AFO limb plantarflexed to a greater degree during push-off (Region 4) than the ankle of the AFO limb (FR leg effect, $p=0.005$; SS leg effect, $p=0.003$). In addition, at SS there was a significant AFO main effect for peak ankle plantarflexion in Regions 1 and 2 (Region 1 AFO effect, $p=0.007$; Region 2 AFO effect, $p=0.014$) while the AFO main effect for peak ankle plantarflexion approached significance at FR (Region 1 AFO effect, $p=0.078$; Region 2 AFO effect, $p=0.087$). Also, at SS the AFO main effect for peak ankle plantarflexion in Region 4 approached significance (AFO effect approached significance, $p=0.052$).

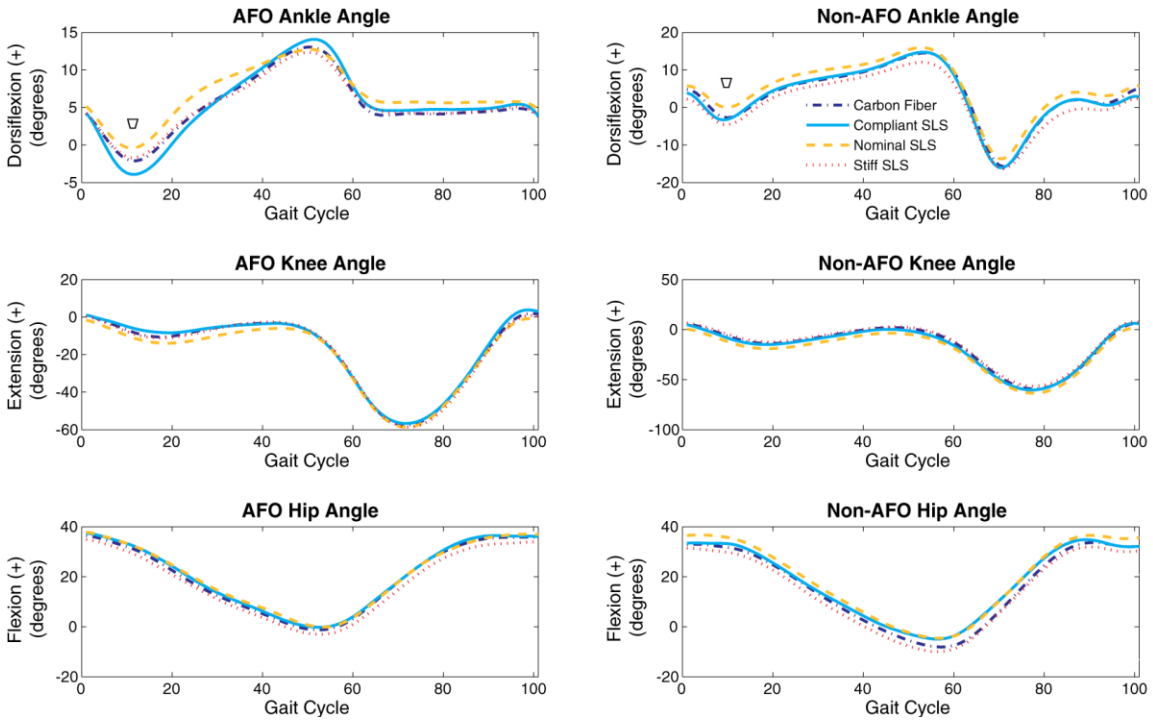

Figure 4. Joint angles for the AFO and non-AFO limbs at the Froude velocity (FR) across the gait cycle. AFO main effects that approach significance are depicted with an open trapezoid (⏢). Significant leg main effects are not shown.

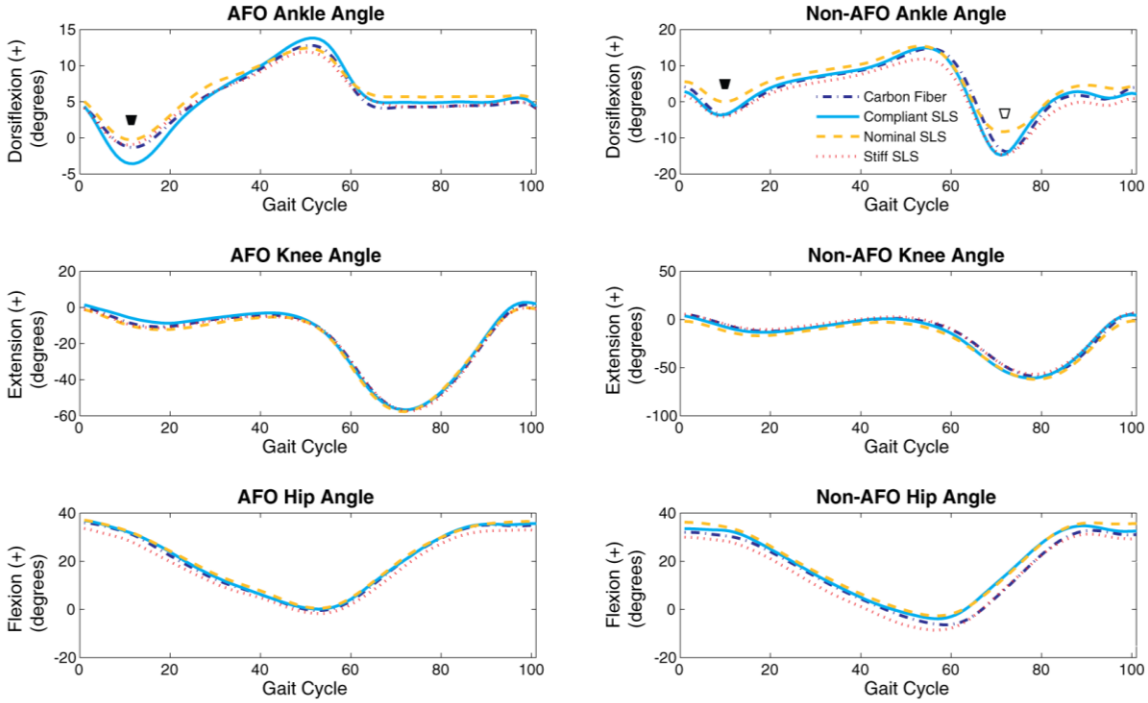

Figure 5. Joint angles for the AFO and non-AFO limbs at the self-selected velocity (SS) across the gait cycle. Significant AFO main effects are depicted with a filled trapezoid (▼) while AFO main effects that approach significance are depicted with an open trapezoid (▽). Significant leg main effects are not shown.

GROUND REACTION FORCE IMPULSES

Decreasing AFO stiffness influenced the GRF impulses during stance (Regions 1 – 4) in both the AFO and non-AFO limbs at both FR (Figure 6) and SS (Figure 7). At both FR and SS, the vertical GRF impulse was significantly larger in the AFO limb compared to the non-AFO limb in Region 1 (FR leg effect, p=0.013; SS leg effect, p=0.029) and significantly larger in the non-AFO limb compared to the AFO limb in Region 2 (FR leg effect, p=0.013; SS leg effect, p=0.015). In Region 4, the propulsive GRF impulse was significantly larger in the non-AFO limb than the AFO limb (FR leg

effect, p=0.011; SS leg effect, p=0.014) and in Region 1 the braking GRF was significantly greater in the AFO limb relative to the non-AFO limb (FR leg effect, p=0.002; SS leg effect, p=0.004).

At FR (Figure 6), the AFO limb vertical GRF impulse in Region 1 was significantly decreased in the CF condition relative to the nominal condition (leg*AFO effect approached significance, p=0.075; CF to nominal, p=0.043) while the decrease in the AFO limb vertical GRF impulse in the compliant condition relative to the nominal condition approached significance (leg*AFO effect approached significance, p=0.075; compliant to nominal, p=0.052). In Region 1, a decrease in the AFO limb braking GRF impulse that approached significance was seen in the CF condition relative to the stiff condition (leg*AFO effect, p=0.011, CF to stiff, p=0.051) and in the compliant condition relative to the stiff condition (leg*AFO effect, p=0.011, compliant to stiff, p=0.053). In addition, the non-AFO limb braking GRF in Region 2 was significantly decreased in the compliant condition compared to the stiff condition (leg*AFO effect, p=0.003, compliant to stiff, p=0.044). In Region 4, the non-AFO limb medial GRF impulse was significantly decreased in the compliant condition relative to the nominal condition (leg*AFO effect approached significance, p=0.079, compliant to nominal, p=0.04).

At SS (Figure 7) the medial GRF impulse in Region 3 was significantly decreased in the compliant condition relative to the stiff condition (AFO effect approached significance, p=0.058, compliant to stiff, p=0.008).

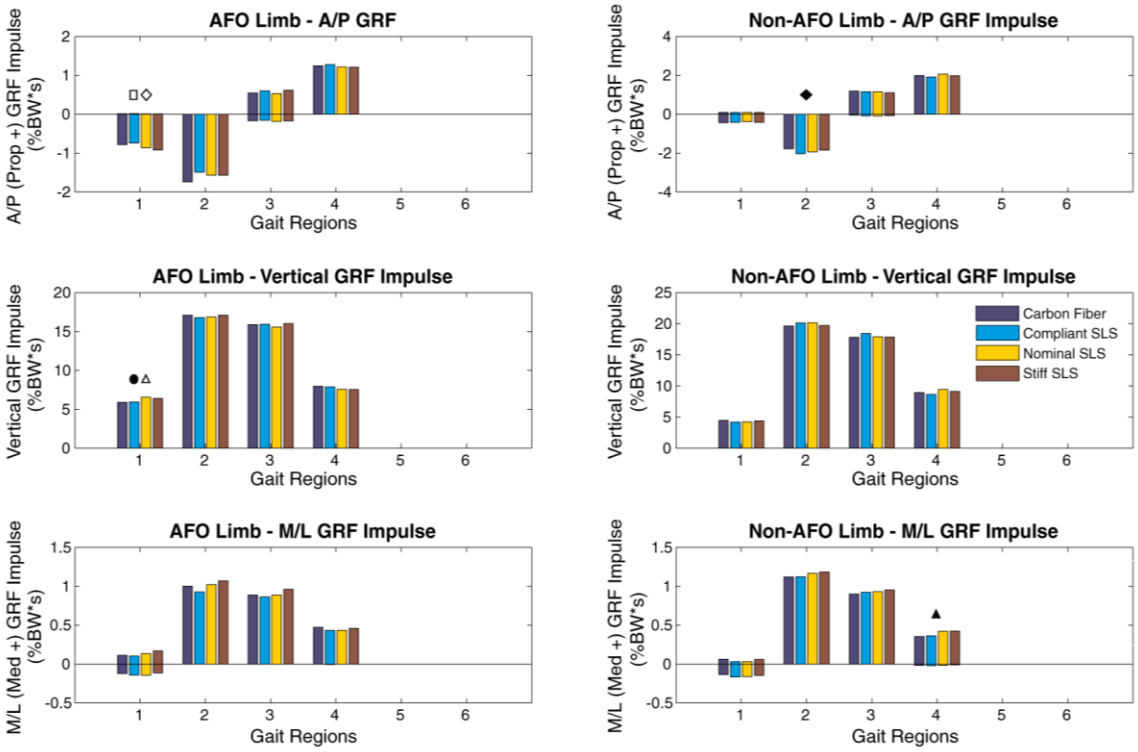

Figure 6. Ground reaction force (GRF) impulses for the AFO and non-AFO limbs at the Froude velocity (FR) across the six regions of the gait cycle: 1) loading, 2) early single-leg support, 3) late single-leg support, 4) push-off, 5) early swing and 6) late swing. Significant differences associated with each GRF impulse quantity are indicated with a filled symbol: carbon fiber to nominal SLS (●), compliant SLS to nominal SLS (▲), and compliant SLS to stiff SLS (◆). Differences that approached significance are indicated with an open symbol: carbon fiber to stiff SLS (□), compliant SLS to nominal SLS (△), and compliant SLS to stiff SLS (◇). Significant leg main effects are not shown.

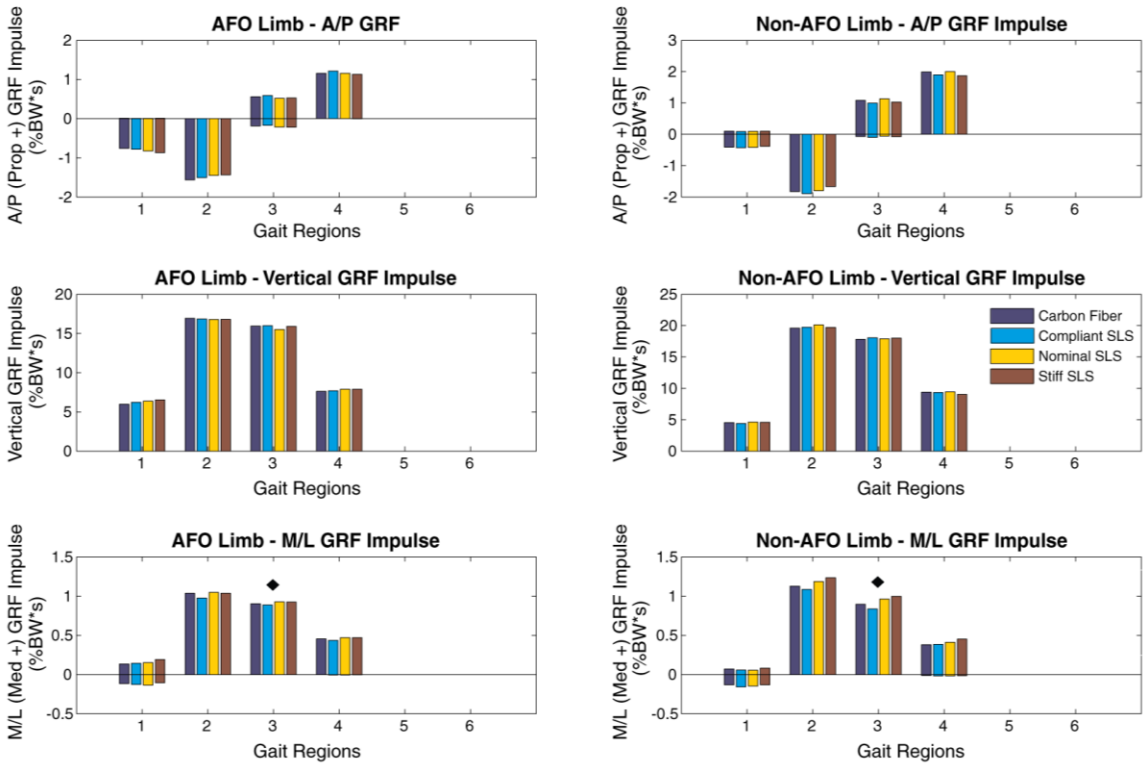

Figure 7. Ground reaction force (GRF) impulses for the AFO and non-AFO limbs at the self-selected velocity (SS) across the six regions of the gait cycle: 1) loading, 2) early single-leg support, 3) late single-leg support, 4) push-off, 5) early swing and 6) late swing. Significant differences between the compliant and stiff SLS AFO conditions are indicated with a filled diamond (◆).

JOINT MOMENTS

Overall, joint moments were only affected by the leg and AFO stiffness condition during loading (Region 1). At both velocities (FR – Figure 8; SS – Figure 9) the non-AFO limb peak hip extensor moment in Region 1 increased significantly compared to the AFO limb peak hip extensor moment (FR leg effect, p=0.02; SS leg effect, p=0.022). Also, at both velocities, the peak knee flexor moment in Region 1 increased (FR leg

effect, p=0.005; SS leg effect, p=0.002) while the peak knee extensor moment in Region 1 decreased (FR leg effect, p=0.019; SS leg effect, p=0.028) in the non-AFO limb's knee relative to the AFO limb's knee. In addition, in Region 1 the peak ankle dorsiflexor moment increased in the AFO limb's ankle compared to the non-AFO limb's ankle (FR leg effect, p=0.021; SS leg effect, p=0.041). At SS, the compliant condition resulted in a significantly smaller peak hip extension moment in Region 1 than the nominal condition (compliant to nominal, p=0.004).

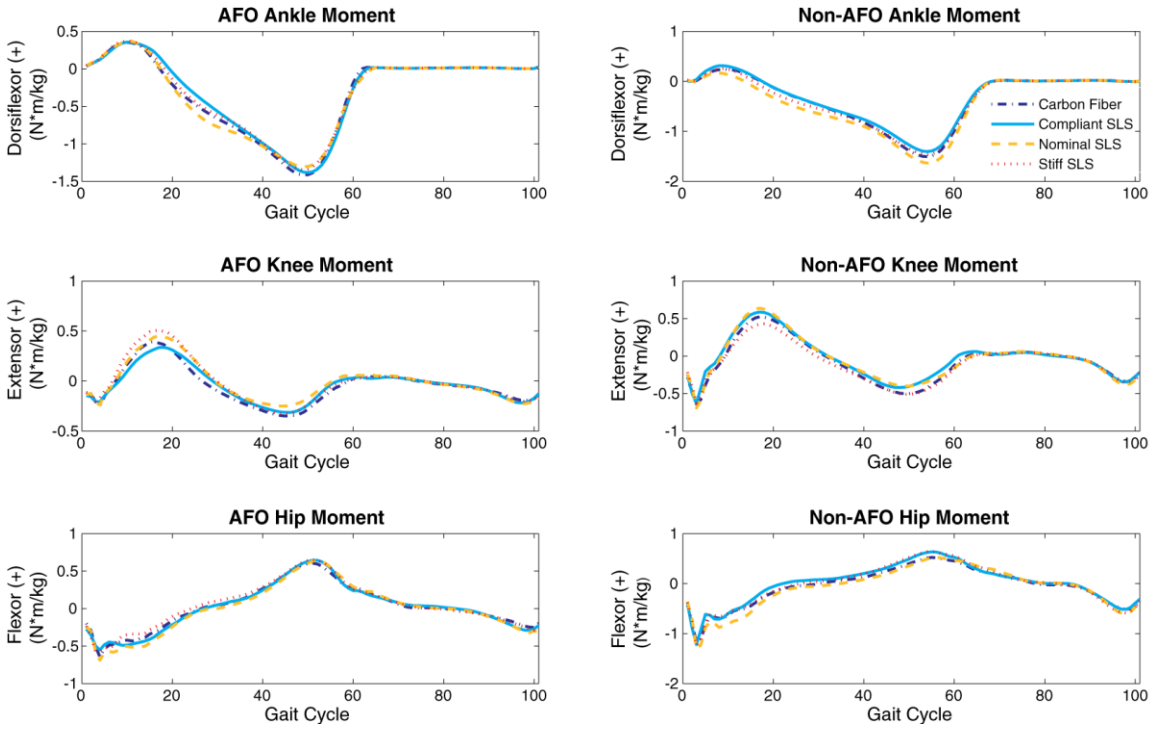

Figure 8. Joint moments for the AFO and non-AFO limbs at the Froude velocity (FR) across the gait cycle. No significant differences between AFO conditions were identified and significant leg main effects are not shown.

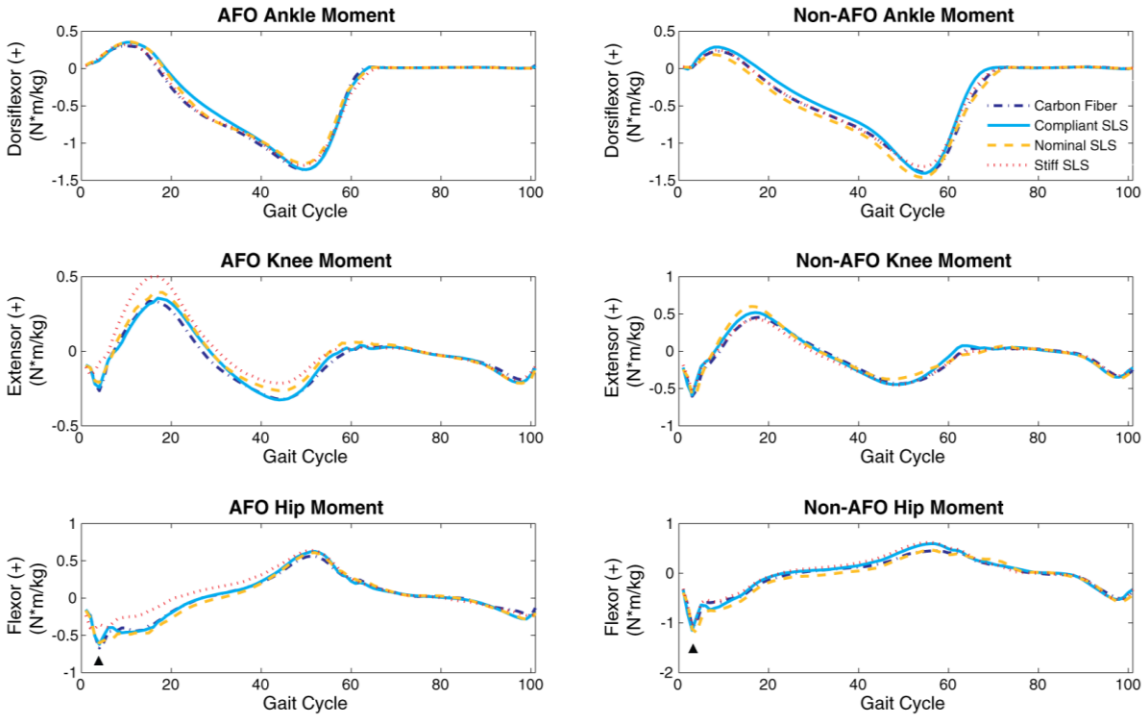

Figure 9. Joint moments for the AFO and non-AFO limbs at the self-selected velocity (SS) across the gait cycle. Significant differences between the compliant and nominal SLS AFO conditions are indicated with a filled diamond (▲). Significant leg main effects are not shown.

JOINT WORK

Decreasing AFO stiffness also influenced the joint work across all regions of the gait cycle in both the AFO and non-AFO limbs and at both the FR (Figure 10) and SS (Figure 11). Overall, significantly greater joint work was performed in the non-AFO limb compared to the AFO limb. At both velocities, significantly greater positive hip work was done in Region 4 at the non-AFO limb's hip compared to the AFO limb's hip (FR leg effect, $p=0.038$; SS leg effect, $p=0.021$). In Region 1, greater positive knee work was done at the non-AFO limb's knee compared to the AFO limb's knee (FR leg effect,

p=0.003; SS leg effect, p=0.003) and in Region 4, greater negative knee work was done at the non-AFO limb's knee compared to the AFO limb's knee (FR leg effect, p=0.021; SS leg effect, p=0.026). In addition, greater positive ankle work was done in Region 4 by the non-AFO limb's ankle relative to the AFO limb's ankle (FR leg effect, $p \leq 0.001$; SS leg effect, p=0.001).

At SS, during early swing (Region 5) the decrease in AFO limb positive hip work in the compliant condition relative to the nominal condition approached significance (leg*AFO effect approached significance, p=0.084; compliant to nominal, p=0.062). At both velocities, a significant interaction effect for negative knee work was identified in Region 1 (FR leg*AFO effect, p=0.041; SS leg*AFO effect, p=0.015), although no pairwise comparisons were significant. At FR, the increase in negative knee work in both limbs in Region 2 in the compliant condition relative to the stiff condition approached significance (compliant to stiff, p=0.068) and at SS the increase in AFO negative knee work in Region 2 in the compliant condition compared to the stiff condition was significant (compliant to stiff, p=0.006).

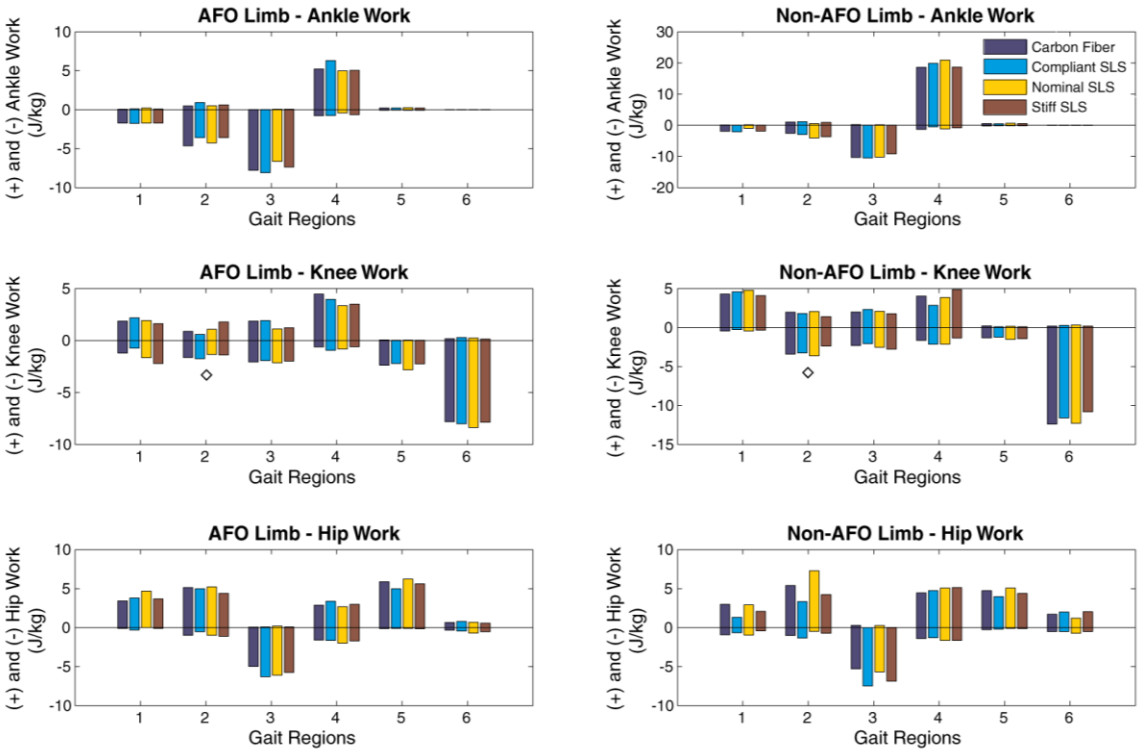

Figure 10. Joint work for the AFO and non-AFO limbs at the Froude velocity (FR) across the six regions of the gait cycle: 1) loading, 2) early single-leg support, 3) late single-leg support, 4) push-off, 5) early swing and 6) late swing. Differences between the compliant and stiff SLS AFOs that approached significance are indicated with an open diamond (◇). Significant leg main effects are not shown.

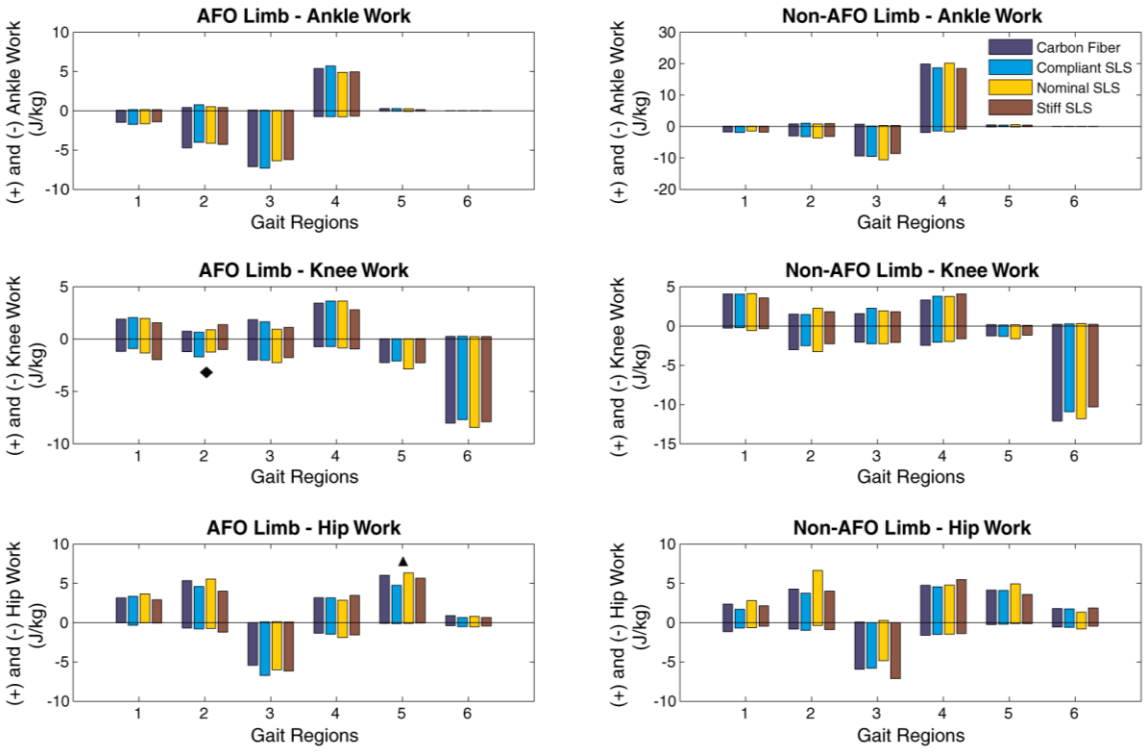

Figure 11. Joint work for the AFO and non-AFO limbs at the self-selected velocity (SS) across the six regions of the gait cycle: 1) loading, 2) early single-leg support, 3) late single-leg support, 4) push-off, 5) early swing and 6) late swing. Significant differences associated with each joint work quantity are indicated with a filled symbol: compliant SLS to nominal SLS (▲), and compliant SLS to stiff SLS (◆). Significant leg main effects are not shown.

Discussion

The overall goal of this study was to use SLS PD-AFOs to identify the relationships between AFO stiffness and gait performance in patients with various lower-limb neuromuscular and musculoskeletal impairments due to limb salvage procedures. The SLS framework enabled the successful generation of AFO struts with predictable and controlled stiffness characteristics (Table 2), similar to previous studies manufacturing ankle-foot prosthetic devices (Fey et al., 2011; Ventura et al., 2011a, b). As expected, the CF and nominal AFOs resulted in some similarities in spatiotemporal gait parameters. However, as a result of decreases in the AFO stiffness, changes in spatiotemporal gait characteristics occurred (Tables A1 and A2). At FR, as stiffness decreased, three of the subjects decreased their average stride width while two of the subjects increased their average step length and decreased their average step time of the AFO limb. In contrast, a previous study that altered the degree of plantarflexion resistance in an AFO found no significant changes in gait velocity (Kobayashi et al., 2012). However, it is not clear if other spatiotemporal gait parameters were influenced in that study as they were not assessed.

In addition to spatiotemporal parameters, decreases in AFO stiffness resulted in altered gait mechanics in both the AFO and non-AFO limbs. At both velocities the non-AFO limb provided increased body support (increased vertical GRF impulse) during early single-leg stance and increased propulsion during push-off compared to the AFO limb. During loading, the AFO limb provided increased body support and increased braking compared to the non-AFO limb at both velocities. Similarly, previous studies of subjects with post-stroke hemiparesis (Allen et al., 2011; Bowden et al., 2006) and lower-limb amputees (Silverman et al., 2008; Zmitrewicz et al., 2006) have found that the non-

impaired limb generates increased propulsion as a compensatory mechanism. In addition, consistent with the results of the current study, previous work has shown that hemiparetic subjects have increased vertical GRFs in the non-paretic limb (Kim and Eng, 2003). In the present study, these changes in the GRF impulses were accompanied by increased joint work in the non-AFO limb relative to the AFO limb. This is consistent with previous studies of hemiparetic subjects (Olney and Richards, 1996; Raja et al., 2012) that suggest subjects increase the magnitude and duration of muscle activity to compensate for the impaired limb.

Unexpectedly, few changes in joint kinematics and kinetics were observed at the ankle as AFO stiffness decreased. No significant changes in ankle work or moments were observed (Figures 8-11). However, several AFO main effects for the ankle angle were observed although no pairwise comparisons reached significance. Thus the hypothesis that ankle ROM and work would increase as stiffness decreased was not supported. This was in contrast with recent studies examining the influence of AFO (Kobayashi et al., 2011, 2012) and prosthetic foot (Fey et al., 2011) stiffness on gait performance which saw significant increases in the ankle range of motion of the AFO or prosthetic limb as stiffness decreased. However, both studies had a larger sample size and thus greater statistical power than the present study. Therefore, it is possible that with a larger sample size the trend of increased ankle ROM in the compliant condition (evident in Figures 4 and 5) could approach significance.

The hypothesis that the AFO's contribution to body support would diminish and knee extensor moments and work would increase to compensate as AFO stiffness decreased was partially supported. During loading at FR, a decrease in body support in the compliant condition compared to the nominal condition approached significance in the AFO limb (Figure 6). In contrast, AFO limb negative knee work in early single-limb

stance increased in the compliant condition compared to the stiff condition at SS and this same trend approached significance at FR (Figures 10 and 11). In addition, at SS the compliant condition resulted in significantly smaller AFO limb and non-AFO limb hip extensor moments during loading than the nominal condition (Figure 9). Thus, although the AFO limb's contribution to body support diminished, the knee extensor moments did not increase. This result is partially consistent with previous studies in amputees that found that as stiffness decreased, the prosthesis contributed less to body support (Fey et al., 2011; Ventura et al., 2011a, b). However, these studies noted an increase in the activity of the knee extensor muscles (Fey et al., 2011; Ventura et al., 2011a, b), which have been previously shown to contribute to body support in unimpaired walking (Anderson and Pandy, 2003; Kepple et al., 1997; Liu et al., 2006; McGowan et al., 2009; Neptune et al., 2004).

Hip extensor muscles (Anderson and Pandy, 2003; Kepple et al., 1997; Liu et al., 2006; McGowan et al., 2009; Neptune et al., 2004) have also been shown to contribute to body support in unimpaired walking. In the present study, although a decrease in body support provided by the AFO limb was observed in the compliant condition, there was not a corresponding increase in the knee and hip extensor joint moments and work. These different results compared to previous studies in amputees suggest that subjects ambulating with an AFO utilize different compensatory mechanisms when stiffness is altered. This difference is likely due to the fact that subjects ambulating with an AFO have two intact limbs, although one is impaired. Previous studies have shown that healthy individuals modulate lower limb joint stiffness, primarily at the ankle, in response to changes in surface stiffness (Farley et al., 1998) or changes in AFO stiffness (Ferris et al., 2006) in order to maintain a constant overall leg stiffness. Although body support decreased as AFO stiffness decreased, similar to the results reported by studies in lower-

limb amputees (Fey et al., 2011; Ventura et al., 2011a, b), the subjects in this study retain some muscle and joint function at the impaired ankle. As a result, these subjects may have been able to partially use the remaining ankle muscles to compensate for this diminished body support by altering joint stiffness. If joint stiffness was increased through a method such as muscle co-contraction, minimal or no changes in joint moments and work would be observed.

Although changes in body support were observed, no significant changes in contribution to forward propulsion were seen as stiffness decreased (Figures 6 and 7). However, during loading of the AFO limb at FR (push-off of the non-AFO limb), a decrease in the AFO limb braking GRF impulse that approached significance was observed in the compliant condition relative to the stiff condition (Figure 6). Reduced braking has been shown to increase net trunk propulsion in the absence of the ankle muscles (Silverman and Neptune, 2012) and although the ankle muscles were still present in the subjects in this study, they were significantly impaired, possibly leading to a similar effect of increased net trunk propulsion from the compliant AFO during push-off due to decreased braking. In addition, at SS the decrease in AFO limb positive hip work during early swing in the compliant condition compared to the nominal condition approached significance, suggesting that more propulsion may have been provided by the compliant AFO in late stance, thus diminishing the work requirement at the hip during push-off and early swing. These results are somewhat similar to recent studies in amputee gait that found evidence to suggest that as stiffness decreased the prosthesis contributed more to forward propulsion (Fey et al., 2011; Ventura et al., 2011a, b), although in this study the AFO limb contributed less to braking. One of these studies (Fey et al., 2011) also found increased peak braking as stiffness decreased, contrary to the results of this study. However, it was postulated that the increase in braking was likely

due to an increase in the activity of the residual and intact knee extensor muscles which have been shown to contribute to body support but also to braking in unimpaired walking (Liu et al., 2006; Neptune et al., 2004). In this study, no significant changes in the knee extensor moment were observed, suggesting that the activity of the knee extensor muscles remained largely unaltered as stiffness decreased and thus did not increase their contribution to braking. In summary, the hypothesis that as stiffness decreased, the AFO's contribution to forward propulsion would increase and hip extensor moments and work would decrease was only minimally supported.

One other notable result was the lack of significant changes in knee and hip angles. A recent study on the effect of AFO plantarflexion resistance on knee joint kinematics showed that increased plantarflexion resistance induced more knee flexion in early stance (Kobayashi et al., 2012), which is in contrast to the present study. Differences between these studies are most likely due to the differences in AFO designs as the current study utilized a passive dynamic AFO while the previous study utilized a hinged oil-damper AFO.

Another noteworthy result occurred in the medial GRF. At FR, during non-AFO push-off (AFO loading) the non-AFO limb medial GRF impulse was significantly decreased in the compliant condition relative to the nominal condition (Figure 6). This was consistent with three of the subjects who decreased their average stride width as stiffness decreased, resulting in diminished medial GRF impulses, and this result highlights the importance of foot placement in mediolateral balance control. At SS during non-AFO late single-limb stance (AFO late swing), the medial GRF impulse was significantly decreased in the compliant condition relative to the stiff condition (Figure 7). In addition, the vertical GRF impulse was larger in the non-AFO limb compared to the AFO limb in early single-limb stance. This may suggest that in preparation for

loading of the AFO limb with the compliant AFO, the subjects shifted more weight to their non-AFO limb, increasing the vertical GRF impulse and decreasing the medial GRF impulse. Overall, this suggests that stability may decrease as AFO stiffness decreases, necessitating increased reliance on the non-AFO limb for stability, specifically during AFO limb loading. This is largely consistent with a recent study which found a correlation between increased prosthesis stiffness and increased dynamic balance control (Nederhand et al., 2012).

Although the results of this study provide insights into the influence of AFO stiffness on gait in individuals with various neuromuscular and musculoskeletal impairments, some potential limitations exist. The primary limitation is the small sample size as data was collected from only six subjects. Having a small sample size decreases statistical power and makes it more difficult to find significant results. Therefore, it is likely that many of the results discussed here that approached significance would become significant if a larger sample size was considered. Thus, future work should focus on collecting data from more subjects to determine the relevance and extension of these results to larger populations. Another potential limitation is that the nominal strut may not have captured all of the functional characteristics of the subject's CF strut, as evidenced by several differences in gait performance between the CF and nominal AFOs. However, as we were interested in the relative changes in these gait parameters as stiffness decreased and we focused on the differences between the three SLS AFO struts, any biasing that did occur due to differences between the CF and nominal AFOs should have been present for all subjects and conditions, and thus the same relative trends would exist.

Another potential limitation is that device acclimation period was not strictly controlled because subjects were given time to acclimate to each new stiffness condition

until they felt comfortable for testing. However, a previous study assessing both healthy subjects and subjects with foot-drop found that changes in lower-limb muscle activity occur almost immediately in response to donning the AFO and do not accumulate over time (Geboers et al., 2002), while another study in amputees showed that changes in temporal parameters and joint kinematics due to altered inertial properties of the prosthesis occurred almost immediately (Smith and Martin, 2011). A similar study in healthy individuals also showed that changes in gait due to asymmetrical lower extremity loading were complete within five minutes of exposure to the load (Smith and Martin, 2007). In the present study, all subjects took a minimum of 30 minutes to acclimate to each new stiffness condition. Thus it is highly likely that all adaptations were complete at the time of testing.

In summary, as AFO stiffness decreased, the AFO limb contributed less to body support and braking. In addition, evidence was found to suggest that stability may decrease as AFO stiffness decreases. Thus, a tradeoff may exist between preserving stability and increasing net propulsion and this tradeoff should be considered when assessing the mobility needs of individuals prescribed PD-AFOs as a result of various neuromuscular and musculoskeletal impairments. However, minimal kinematic and kinetic compensations to this reduced body support, braking and stability, occurred. Future work should focus on analyzing individual muscle activity to determine if individual muscle compensations occurred that were not evident in the net joint moment and work quantities, such as increased muscle co-contraction to increase joint stiffness and maintain overall leg stiffness.

Appendix

Table A1. Spatial gait parameters for all six subjects collected for each condition – Carbon Fiber (CF), Nominal SLS, Compliant SLS, and Stiff SLS struts – at each velocity – Froude velocity (FR) and self-selected velocity (SS). 'AFO' represents the AFO limb and 'No AFO' represents the non-AFO limb.

			Average Stride Width (m)	Average Stride Length (m)	Average Step Length (m)	
					AFO	No AFO
Subject 1	CF	FR	0.117	1.597	0.798	0.795
		SS	0.138	1.667	0.814	0.849
	Nominal	FR	0.125	1.628	0.814	0.812
		SS	0.118	1.750	0.876	0.872
	Compliant	FR	0.104	1.640	0.818	0.824
		SS	0.117	1.737	0.843	0.886
	Stiff	FR	0.128	1.636	0.793	0.832
		SS	0.129	1.707	0.836	0.851
Subject 2	CF	FR	0.180	1.480	0.779	0.694
		SS	0.183	1.314	0.685	0.629
	Nominal	FR	0.217	1.351	0.697	0.666
		SS	0.219	1.293	0.665	0.638
	Compliant	FR	0.208	1.457	0.771	0.695
		SS	0.187	1.278	0.663	0.622
	Stiff	FR	0.174	1.450	0.726	0.725
		SS	0.194	1.235	0.627	0.619
Subject 3	CF	FR	0.135	1.525	0.870	0.637
		SS	0.129	1.322	0.745	0.585
	Nominal	FR	0.115	1.562	0.933	0.636
		SS	0.123	1.262	0.785	0.492
	Compliant	FR	0.133	1.436	0.795	0.646

	Stiff	SS	0.133	1.343	0.757	0.603
		FR	0.148	1.463	0.868	0.605
		SS	0.140	1.256	0.738	0.533
Subject 4	CF	FR	0.133	1.524	0.734	0.783
		SS	0.122	1.423	0.699	0.729
	Nominal	FR	0.126	1.513	0.750	0.771
		SS	0.129	1.481	0.708	0.758
	Compliant	FR	0.128	1.444	0.724	0.742
		SS	0.143	1.420	0.703	0.737
	Stiff	FR	0.136	1.466	0.736	0.742
		SS	0.144	1.503	0.770	0.748
Subject 5	CF	FR	0.120	1.352	0.684	0.673
		SS	0.136	1.419	0.719	0.711
	Nominal	FR	0.110	1.398	0.705	0.696
		SS	0.129	1.390	0.710	0.681
	Compliant	FR	0.107	1.407	0.716	0.686
		SS	0.122	1.337	0.677	0.673
	Stiff	FR	0.124	1.402	0.709	0.698
		SS	0.125	1.364	0.684	0.686
Subject 6	CF	FR	0.155	1.563	0.808	0.755
		SS	0.153	1.674	0.856	0.826
	Nominal	FR	0.167	1.580	0.832	0.742
		SS	0.159	1.621	0.843	0.780
	Compliant	FR	0.148	1.618	0.851	0.756
		SS	0.153	1.637	0.871	0.781
	Stiff	FR	0.170	1.551	0.767	0.773
		SS	0.156	1.579	0.828	0.766

Table A2. Temporal gait parameters for all six subjects collected for each condition – Carbon Fiber (CF), Nominal SLS, Compliant SLS, and Stiff SLS – at each speed – Froude (FR) and self-selected (SSWV). 'AFO' represents the AFO limb and 'No AFO' represents the non-AFO limb.

			Average Step Time (sec)		**Average Stance Time (sec)**		**Average Swing Time (sec)**		**Average Stride Time (sec)**	**Average Double Support Time (sec)**	**Average Speed (m/s)**
			AFO	No AFO	AFO	No AFO	AFO	No AFO			
Subject 1	CF	FR	0.638	0.623	0.763	0.823	0.518	0.433	1.269	0.324	1.259
		SS	0.598	0.588	0.700	0.775	0.495	0.412	1.191	0.288	1.400
	Nominal	FR	0.612	0.572	0.690	0.778	0.495	0.413	1.188	0.283	1.370
		SS	0.583	0.542	0.643	0.725	0.480	0.403	1.126	0.247	1.554
	Compliant	FR	0.623	0.603	0.722	0.793	0.497	0.418	1.215	0.293	1.350
		SS	0.578	0.568	0.672	0.740	0.482	0.407	1.150	0.265	1.511
	Stiff	FR	0.632	0.600	0.732	0.808	0.503	0.438	1.241	0.303	1.319
		SS	0.620	0.588	0.713	0.773	0.502	0.432	1.210	0.278	1.411
Subject 2	CF	FR	0.570	0.587	0.717	0.723	0.465	0.443	1.174	0.277	1.260
		SS	0.597	0.617	0.758	0.782	0.473	0.432	1.223	0.322	1.075
	Nominal	FR	0.523	0.588	0.698	0.710	0.417	0.410	1.118	0.289	1.209
		SS	0.535	0.592	0.702	0.727	0.422	0.407	1.128	0.301	1.146
	Compliant	FR	0.558	0.602	0.717	0.725	0.450	0.427	1.159	0.279	1.257
		SS	0.590	0.635	0.763	0.787	0.463	0.433	1.223	0.326	1.045
	Stiff	FR	0.537	0.587	0.695	0.707	0.428	0.430	1.130	0.283	1.283
		SS	0.563	0.632	0.767	0.775	0.440	0.423	1.203	0.346	1.027
Subject 3	CF	FR	0.605	0.470	0.618	0.730	0.478	0.353	1.090	0.268	1.400
		SS	0.705	0.532	0.717	0.875	0.517	0.357	1.233	0.357	1.073
	Nominal	FR	0.605	0.472	0.603	0.732	0.475	0.343	1.077	0.261	1.451

	Compliant	SS	0.703	0.507	0.700	0.868	0.512	0.338	1.209	0.360	1.043
		FR	0.650	0.512	0.667	0.792	0.488	0.377	1.162	0.296	1.237
	Stiff	SS	0.677	0.535	0.703	0.840	0.508	0.380	1.216	0.331	1.105
		FR	0.627	0.463	0.618	0.750	0.488	0.347	1.102	0.278	1.328
		SS	0.705	0.520	0.720	0.873	0.510	0.360	1.232	0.366	1.020
Subject 4	CF	FR	0.488	0.535	0.627	0.625	0.410	0.397	1.029	0.229	1.481
		SS	0.517	0.587	0.693	0.675	0.412	0.415	1.098	0.268	1.297
	Nominal	FR	0.503	0.550	0.640	0.638	0.422	0.413	1.057	0.231	1.432
		SS	0.508	0.558	0.658	0.658	0.418	0.418	1.077	0.250	1.376
	Compliant	FR	0.532	0.535	0.632	0.663	0.433	0.408	1.068	0.228	1.351
		SS	0.542	0.533	0.643	0.687	0.432	0.413	1.088	0.244	1.307
	Stiff	FR	0.513	0.548	0.647	0.653	0.413	0.402	1.058	0.235	1.386
		SS	0.512	0.537	0.633	0.647	0.412	0.400	1.046	0.230	1.437
Subject 5	CF	FR	0.558	0.547	0.663	0.688	0.440	0.417	1.104	0.250	1.225
		SS	0.545	0.535	0.645	0.668	0.435	0.415	1.082	0.229	1.312
	Nominal	FR	0.553	0.547	0.657	0.693	0.440	0.407	1.098	0.253	1.273
		SS	0.552	0.532	0.645	0.678	0.435	0.401	1.084	0.238	1.282
	Compliant	FR	0.547	0.525	0.640	0.675	0.438	0.417	1.085	0.239	1.296
		SS	0.573	0.567	0.677	0.718	0.453	0.422	1.135	0.256	1.178
	Stiff	FR	0.555	0.548	0.648	0.688	0.455	0.415	1.103	0.238	1.270
		SS	0.562	0.553	0.663	0.697	0.450	0.417	1.104	0.250	1.225
Subject 6	CF	FR	0.695	0.635	0.788	0.848	0.547	0.475	1.329	0.302	1.176
		SS	0.640	0.554	0.663	0.762	0.506	0.440	1.185	0.243	1.413
	Nominal	FR	0.655	0.590	0.738	0.800	0.517	0.460	1.258	0.290	1.256
		SS	0.643	0.575	0.710	0.780	0.508	0.443	1.221	0.262	1.328
	Compliant	FR	0.648	0.607	0.755	0.788	0.535	0.453	1.266	0.283	1.279
		SS	0.657	0.598	0.730	0.787	0.510	0.452	1.239	0.280	1.321
	Stiff	FR	0.700	0.667	0.810	0.845	0.558	0.532	1.373	0.308	1.130
		SS	0.652	0.598	0.730	0.792	0.515	0.455	1.246	0.282	1.267

References

Allen, J.L., Kautz, S.A., Neptune, R.R., 2011. Step length asymmetry is representative of compensatory mechanisms used in post-stroke hemiparetic walking. Gait Posture 33, 538-543.

Allen, J.L., Neptune, R.R., 2012. Three-dimensional modular control of human walking. J Biomech 45, 2157-2163.

Anderson, F.C., Pandy, M.G., 2003. Individual muscle contributions to support in normal walking. Gait Posture 17, 159-169.

Baker, R., 2001. Pelvic angles: a mathematically rigorous definition which is consistent with a conventional clinical understanding of the terms. Gait Posture 13, 1-6.

Bartonek, A., Eriksson, M., Gutierrez-Farewik, E.M., 2007. Effects of carbon fibre spring orthoses on gait in ambulatory children with motor disorders and plantarflexor weakness. Dev Med Child Neurol 49, 615-620.

Bleyenheuft, C., Caty, G., Lejeune, T., Detrembleur, C., 2008. Assessment of the Chignon dynamic ankle-foot orthosis using instrumented gait analysis in hemiparetic adults. Ann Readapt Med Phys 51, 154-160.

Bowden, M.G., Balasubramanian, C.K., Neptune, R.R., Kautz, S.A., 2006. Anterior-posterior ground reaction forces as a measure of paretic leg contribution in hemiparetic walking. Stroke 37, 872-876.

Bregman, D.J., De Groot, V., Van Diggele, P., Meulman, H., Houdijk, H., Harlaar, J., 2010. Polypropylene ankle foot orthoses to overcome drop-foot gait in central neurological patients: a mechanical and functional evaluation. Prosthet Orthot Int 34, 293-304.

Bregman, D.J., van der Krogt, M.M., de Groot, V., Harlaar, J., Wisse, M., Collins, S.H., 2011. The effect of ankle foot orthosis stiffness on the energy cost of walking: a simulation study. Clin Biomech (Bristol, Avon) 26, 955-961.

Buckon, C.E., Thomas, S.S., Jakobson-Huston, S., Moor, M., Sussman, M., Aiona, M., 2004. Comparison of three ankle-foot orthosis configurations for children with spastic diplegia. Dev Med Child Neurol 46, 590-598.

Buckon, C.E., Thomas, S.S., Jakobson-Huston, S., Sussman, M., Aiona, M., 2001. Comparison of three ankle-foot orthosis configurations for children with spastic hemiplegia. Dev Med Child Neurol 43, 371-378.

Collins, T.D., Ghoussayni, S.N., Ewins, D.J., Kent, J.A., 2009. A six degrees-of-freedom marker set for gait analysis: repeatability and comparison with a modified Helen Hayes set. Gait Posture 30, 173-180.

Danielsson, A., Sunnerhagen, K.S., 2004. Energy expenditure in stroke subjects walking with a carbon composite ankle foot orthosis. J Rehabil Med 36, 165-168.

de Wit, D.C., Buurke, J.H., Nijlant, J.M., Ijzerman, M.J., Hermens, H.J., 2004. The effect of an ankle-foot orthosis on walking ability in chronic stroke patients: a randomized controlled trial. Clin Rehabil 18, 550-557.

Desloovere, K., Molenaers, G., Van Gestel, L., Huenaerts, C., Van Campenhout, A., Callewaert, B., Van de Walle, P., Seyler, J., 2006. How can push-off be preserved during use of an ankle foot orthosis in children with hemiplegia? A prospective controlled study. Gait Posture 24, 142-151.

Dvorznak, M., Fitzpatrick, L., Karmarkar, A., Kelleher, A., McCann, T., 2007. Orthotic devices, in: Rory A Cooper, H.O., Douglas A Hobson (Ed.), An Introduction to Rehabilitation Engineering. Taylor & Francis Group, New York, pp. 261-285.

Farley, C.T., Houdijk, H.H., Van Strien, C., Louie, M., 1998. Mechanism of leg stiffness adjustment for hopping on surfaces of different stiffnesses. J Appl Physiol 85, 1044-1055.

Faustini, M.C., Neptune, R.R., Crawford, R.H., Rogers, W.E., Bosker, G., 2006. An experimental and theoretical framework for manufacturing prosthetic sockets for transtibial amputees. IEEE Transactions on Neural Systems and Rehabilitation Engineering 14, 304-310.

Faustini, M.C., Neptune, R.R., Crawford, R.H., Stanhope, S.J., 2008. Manufacture of passive dynamic ankle-foot orthoses using selective laser sintering. IEEE Trans Biomed Eng 55, 784-790.

Ferris, D.P., Bohra, Z.A., Lukos, J.R., Kinnaird, C.R., 2006. Neuromechanical adaptation to hopping with an elastic ankle-foot orthosis. J Appl Physiol 100, 163-170.

Fey, N.P., Klute, G.K., Neptune, R.R., 2011. The influence of energy storage and return foot stiffness on walking mechanics and muscle activity in below-knee amputees. Clin Biomech (Bristol, Avon) 26, 1025-1032.

Geboers, J.F., Drost, M.R., Spaans, F., Kuipers, H., Seelen, H.A., 2002. Immediate and long-term effects of ankle-foot orthosis on muscle activity during walking: a randomized study of patients with unilateral foot drop. Arch Phys Med Rehabil 83, 240-245.

Gok, H., Kucukdeveci, A., Altinkaynak, H., Yavuzer, G., Ergin, S., 2003. Effects of ankle-foot orthoses on hemiparetic gait. Clin Rehabil 17, 137-139.

Goldberg, B., Hsu, J.D., 1997. Atlas of orthoses and assistive devices, Third ed. Mosby-Year Book, Inc., p. 720.

Grood, E.S., Suntay, W.J., 1983. A joint coordinate system for the clinical description of three-dimensional motions: application to the knee. J Biomech Eng 105, 136-144.

Kepple, T.M., Siegel, K.L., Stanhope, S.J., 1997. Relative contributions of the lower extremity joint moments to forward progression and support during gait. Gait Posture 6, 1-8.

Kim, C.M., Eng, J.J., 2003. Symmetry in vertical ground reaction force is accompanied by symmetry in temporal but not distance variables of gait in persons with stroke. Gait Posture 18, 23-28.

Kobayashi, T., Leung, A.K., Akazawa, Y., Hutchins, S.W., 2011. Design of a stiffness-adjustable ankle-foot orthosis and its effect on ankle joint kinematics in patients with stroke. Gait Posture 33, 721-723.

Kobayashi, T., Leung, A.K., Akazawa, Y., Hutchins, S.W., 2012. The effect of varying the plantarflexion resistance of an ankle-foot orthosis on knee joint kinematics in patients with stroke. Gait Posture.

Lehmann, J.F., Condon, S.M., de Lateur, B.J., Price, R., 1986. Gait abnormalities in peroneal nerve paralysis and their corrections by orthoses: a biomechanical study. Arch Phys Med Rehabil 67, 380-386.

Lehmann, J.F., Condon, S.M., de Lateur, B.J., Smith, J.C., 1985. Ankle-foot orthoses: effect on gait abnormalities in tibial nerve paralysis. Arch Phys Med Rehabil 66, 212-218.

Liu, M.Q., Anderson, F.C., Pandy, M.G., Delp, S.L., 2006. Muscles that support the body also modulate forward progression during walking. J Biomech 39, 2623-2630.

Manal, K., McClay, I., Stanhope, S., Richards, J., Galinat, B., 2000. Comparison of surface mounted markers and attachment methods in estimating tibial rotations during walking: an in vivo study. Gait Posture 11, 38-45.

McGowan, C.P., Kram, R., Neptune, R.R., 2009. Modulation of leg muscle function in response to altered demand for body support and forward propulsion during walking. J Biomech 42, 850-856.

Nederhand, M.J., Van Asseldonk, E.H., van der Kooij, H., Rietman, H.S., 2012. Dynamic balance control (DBC) in lower leg amputee subjects; contribution of the regulatory activity of the prosthesis side. Clin Biomech (Bristol, Avon) 27, 40-45.

Neptune, R.R., Kautz, S.A., Zajac, F.E., 2001. Contributions of the individual ankle plantar flexors to support, forward progression and swing initiation during walking. J Biomech 34, 1387-1398.

Neptune, R.R., Zajac, F.E., Kautz, S.A., 2004. Muscle force redistributes segmental power for body progression during walking. Gait Posture 19, 194-205.

Olney, S.J., Richards, C., 1996. Hemiparetic gait following stroke. Part I: characteristics. Gait Posture 4, 136-148.

Pallari, J.H., Dalgarno, K.W., Woodburn, J., 2010. Mass customization of foot orthoses for rheumatoid arthritis using selective laser sintering. IEEE Trans Biomed Eng 57, 1750-1756.

Pandy, M.G., Lin, Y.C., Kim, H.J., 2010. Muscle coordination of mediolateral balance in normal walking. J Biomech 43, 2055-2064.

Patzkowski, J.C., Blanck, R.V., Owens, J.G., Wilken, J.M., Kirk, K.L., Wenke, J.C., Hsu, J.R., 2012. Comparative effect of orthosis design on functional performance. J Bone Joint Surg Am 94, 507-515.

Raja, B., Neptune, R.R., Kautz, S.A., 2012. Coordination of the non-paretic leg during hemiparetic gait: expected and novel compensatory patterns. Clin Biomech (Bristol, Avon) 27, 1023-1030.

Ramstrand, N., Ramstrand, S., 2010. AAOP state-of-the-science evidence report: the effect of ankle-foot orthoses on balance - a systematic review, The effect of ankle foot orthoses (AFOs) on balance. Journal of Prosthetics and Orthotics, pp. 4-23.

Rogers, B., Bosker, G., Faustini, M., Walden, G., Neptune, R.R., Crawford, R., 2008. Case report: variably compliant transtibial prosthetic socket fabricated using solid freeform fabrication. Journal of Prosthetics and Orthotics 20, 1-7.

Rogers, B., Bosker, G.W., Crawford, R.H., Faustini, M.C., Neptune, R.R., Walden, G., Gitter, A.J., 2007. Advanced Trans-Tibial Socket Fabrication Using Selective Laser Sintering. Prosthetics and Orthotics International 31, 88-100.

Schrank, E.S., Stanhope, S.J., 2011. Dimensional accuracy of ankle-foot orthoses constructed by rapid customization and manufacturing framework. J Rehabil Res Dev 48, 31-42.

Silverman, A.K., Fey, N.P., Portillo, A., Walden, J.G., Bosker, G., Neptune, R.R., 2008. Compensatory mechanisms in below-knee amputee gait in response to increasing steady-state walking speeds. Gait Posture 28, 602-609.

Silverman, A.K., Neptune, R.R., 2012. Muscle and prosthesis contributions to amputee walking mechanics: a modeling study. J Biomech 45, 2271-2278.

Smith, J.D., Martin, P.E., 2007. Walking patterns change rapidly following asymmetrical lower extremity loading. Hum Mov Sci 26, 412-425.

Smith, J.D., Martin, P.E., 2011. Short and longer term changes in amputee walking patterns due to increased prosthesis inertia. Journal of Prosthetics and Orthotics 23, 114-123.

Tyson, S.F., Thornton, H.A., 2001. The effect of a hinged ankle foot orthosis on hemiplegic gait: objective measures and users' opinions. Clin Rehabil 15, 53-58.

Van Gestel, L., Molenaers, G., Huenaerts, C., Seyler, J., Desloovere, K., 2008. Effect of dynamic orthoses on gait: a retrospective control study in children with hemiplegia. Dev Med Child Neurol 50, 63-67.

Vaughan, C.L., O'Malley, M.J., 2005. Froude and the contribution of naval architecture to our understanding of bipedal locomotion. Gait Posture 21, 350-362.

Ventura, J.D., Klute, G.K., Neptune, R.R., 2011a. The effect of prosthetic ankle energy storage and return properties on muscle activity in below-knee amputee walking. Gait Posture 33, 220-226.

Ventura, J.D., Klute, G.K., Neptune, R.R., 2011b. The effects of prosthetic ankle dorsiflexion and energy return on below-knee amputee leg loading. Clin Biomech (Bristol, Avon) 26, 298-303.

Wilken, J.M., Rodriguez, K.M., Brawner, M., Darter, B.J., 2012. Reliability and minimal detectible change values for gait kinematics and kinetics in healthy adults. Gait Posture 35, 301-307.

Wolf, S.I., Alimusaj, M., Rettig, O., Doderlein, L., 2008. Dynamic assist by carbon fiber spring AFOs for patients with myelomeningocele. Gait Posture 28, 175-177.

Wu, G., Cavanagh, P.R., 1995. ISB recommendations for standardization in the reporting of kinematic data. J Biomech 28, 1257-1261.

Wu, G., Siegler, S., Allard, P., Kirtley, C., Leardini, A., Rosenbaum, D., Whittle, M., D'Lima, D.D., Cristofolini, L., Witte, H., Schmid, O., Stokes, I., 2002. ISB recommendation on definitions of joint coordinate system of various joints for the reporting of human joint motion—part I: ankle, hip, and spine. J Biomech 35, 543-548.

Yamamoto, S., Ebina, M., Kubo, S., Hayashi, T., Akita, Y., Hayakawa, Y., 1999. Development of a new ankle-foot orthosis with dorsiflexion assist, part 2: structure and evaluation. Journal of Prosthetics and Orthotics 11, 24-28.

Yamamoto, S., Hagiwara, A., Mizobe, T., Yokoyama, O., Yasui, T., 2005. Development of an ankle-foot orthosis with an oil damper. Prosthet Orthot Int 29, 209-219.

Yokoyama, O., Sashika, H., Hagiwara, A., Yamamoto, S., Yasui, T., 2005. Kinematic effects on gait of a newly designed ankle-foot orthosis with oil damper resistance: a case series of 2 patients with hemiplegia. Arch Phys Med Rehabil 86, 162-166.

Zmitrewicz, R.J., Neptune, R.R., Walden, J.G., Rogers, W.E., Bosker, G.W., 2006. The effect of foot and ankle prosthetic components on braking and propulsive impulses during transtibial amputee gait. Arch Phys Med Rehabil 87, 1334-1339.

Vita

Nicole Lynn Guckert was raised in Austin, Texas and graduated salutatorian from James Bowie High School in May, 2006. She attended the University of Texas at Austin where she graduated with a Bachelor of Science in Biomedical Engineering with Highest Honors from the Cockrell School of Engineering in May 2010. While pursuing her undergraduate degree, she was a research assistant in the Laboratory for Cellular and Macromolecular Engineering under the direction of Dr. Krishnendu Roy at the University of Texas at Austin. In addition, she was an intern at Apollo Endosurgery, a small medical device company. Nicole was accepted into graduate school at the University of Texas at Austin in the Mechanical Engineering Department and joined the Neuromuscular Biomechanics Laboratory under the direction of Dr. Richard Neptune in August 2010.

Permanent email address: nicole.guckert@gmail.com

This thesis was typed by the author.